

Origin of particulate matter pollution episodes in wintertime over the Paris Basin

B. Bessagnet^{a,*}, A. Hodzic^b, O. Blanchard^a, M. Lattuati^c, O. Le Bihan^a,
H. Marfaing^c, L. Rouil^a

^a*Institut National de l'Environnement Industriel et des Risques, INERIS, Parc Technologique ALATA-B.P. No. 2,
60550 Verneuil en Halatte, France*

^b*Laboratoire de Météorologie Dynamique, Ecole Polytechnique 91128 Palaiseau, France*

^c*AIRPARIF, Surveillance de la qualité de l'air en Ile-de-France, 7 rue Crillon 75004, Paris, France*

Received 12 January 2005; received in revised form 17 June 2005; accepted 27 June 2005

Abstract

Several wintertime pollution events due to particulate matter on the Paris Basin in 2003 are investigated in this paper. High-pressure systems close to Scandinavia or the North Sea involve highly stable conditions with slight Northeasterly flux on France leading to high airborne pollutant concentrations. An evaluation of the CHIMERE model results against observations over the Paris area is proposed. While PM₁₀, nitrate and ammonium seem fairly well reproduced, sulfate concentrations remain difficult to predict. A specific study, by removing Ile-de-France emissions, displays on 21 February and 21 March episodes an important ammonium nitrate contribution, mainly originating from outside the Paris area. According to the model results, the Paris Basin has also a large influence up to the Southwest of France. In a similar way, an investigation of the possible sources outside the Paris basin, displays a strong influence of emissions from Germany, the Netherlands and Belgium during these episodes. To a lesser extent, Italy has an influence on the Paris area at the end of the episodes. It is also demonstrated that in some situations, the contribution of locally produced or emitted particles is prevalent at the ground level. The influence of French emissions is also studied from 20 to 25 March displaying an influence on Spain and a strong impact at the end of the episode successively on Great Britain, Belgium, the Netherlands when winds veer Southeast and West. This influence is also significant up to Eastern Europe.

© 2005 Elsevier Ltd. All rights reserved.

Keywords: Modeling study; Aerosols; Episodes; Model evaluation; Emission inventory; Ammonium nitrate

1. Introduction

At the global scale, particles act on climate by affecting the Earth's radiative balance; altering the

scattering properties of the atmosphere (direct impact), and changing cloud properties (indirect impact). Visibility impairment, as a result of scattering and absorption of light by particles, is another problem due to particulate matter (PM) pollution. Particles in the atmosphere have recently received much interest because of increasing epidemiological and experimental evidence of their impact on human health (Katsouyanni et al., 1997; WHO, 2003; Pope et al., 2002; EPA, 2004).

*Corresponding author. Tel.: 33 344 55 65 33;
fax: 33 344 55 68 99.

E-mail address: bertrand.bessagnet@ineris.fr
(B. Bessagnet).

Since most people live in large city areas, focusing at the urban scale allows for a better evaluation of the exposure of their inhabitants. Although PM measurements have been deployed in most cities, the modeling approach is essential at local scales in order to investigate processes leading to PM pollution episodes and to predict their concentration levels. Modeling tools are also used to study emission control scenarios. Seigneur (2001) reviews the current status of the mathematical modeling of atmospheric PM and the ability of such tools to simulate pollution episodes. This review suggests that several models (Jacobson, 1997; Pai et al., 2000; Ackermann et al., 1998; Meng et al., 1998) provide a fairly comprehensive treatment of the major processes, but the author states that some uncertainties remain. For the CHIMERE model Bessagnet et al. (2004) reported a complete panel of error statistics for rural stations in Europe, and Hodzic et al. (2005) proposed a similar evaluation over the Paris Basin. These analyses were performed over an entire year to get representative results. They showed the ability of the CHIMERE model to deal with the simulation of atmospheric aerosol components.

The topic of this paper is to study several wintertime PM pollution episodes over the Paris Basin at the continental and local scales. In France, high-pressure systems in the North of Europe give highly stable and windless atmospheric conditions, sometimes favoring the advection of very cold air masses from Central Europe. These situations lead to strong PM pollution episodes over the North of France. Hereafter, three wintertime episodes occurring in February and March 2003 over the Paris basin are studied with the CHIMERE model. Two PM measurement systems, TEOM and PARTISOL, are available to get data to assess model performances. The TEOM instrument is routinely used to get continuous measurements. However, artifacts may occur during the conditioning procedure (sample heated at 50 °C) due to the volatilization of PM components such as ammonium nitrate (Allen et al., 1997) or semi-volatile organic species. To avoid and to quantify the TEOM measurement uncertainties, the gravimetric method PARTISOL is used. PARTISOL filters are analyzed to determine sulfate, nitrate and ammonium concentrations. Due to instrumental constraints, only daily measurements are available with the PARTISOL system. These data are used to evaluate the model at two sites near Paris. The question of the origin of these high PM concentrations during the episodes is addressed. The respective contribution of PM production by local sources and long-range transport is investigated. A sensitivity analysis on the emission inventories is proposed to understand the impact of Paris area and neighboring country emissions on PM concentrations observed during these episodes. The influence of French emissions on the rest of Europe is also discussed.

2. Model setup

In this study, the regional version (V200501G) of the Chemistry Transport Model, CHIMERE, applied over Europe (Schmidt et al., 2001; Bessagnet et al., 2004; Vautard et al., 2005) is used to constrain a local version applied over the Ile-de-France area (Hodzic et al., 2005). The model grid at the European scale ranges from 10.5°W to 22.5°E and from 35°N to 57.5°N with a $\frac{1}{2}$ degree resolution both in latitude and longitude. The domain covers most of the Western Europe and the Western Mediterranean basin. The Ile-de-France sub-domain grid covers the Paris Basin with a 5 km resolution. The vertical grid contains eight layers from surface to 500 hPa. The dynamics and gas-phase parts of the model are described in Schmidt et al. (2001) with recent improvements reported in Vautard et al. (2003). The aerosol module is presented in Bessagnet et al. (2004) and Bessagnet and Rosset (2001). The full model documentation for the updated version can be found via the internet at: <http://euler.lmd.polytechnique.fr/chimere>.

In this version, particles are assumed to be composed of seven chemical species: primary particle material (PPM), desert dust, (dust) anthropogenic and biogenic secondary organic aerosol (SOA), sulfate, nitrate, ammonium and water. Sea salts are not considered in this exercise, this species has only an influence on coastal regions. PPM includes not only anthropogenic s but also biogenic particles like vegetative debris, insects, plant waxes and particles produced by soil erosion (detailed in Vautard et al., 2005). These latter species are expected to be negligible in winter (due to high soil humidity). In this version, particle diameters are described by 11 bins ranging from 10 nm to 20 μ m. The model accounts for the coagulation process as described in Gelbard and Seinfeld (1980), and Warren (1986). The dynamics of the absorption process of organic and inorganic semi-volatile species is parameterized with a first-order equation. For the ternary system, sulfate/nitrate/ammonium, the thermodynamic equilibrium is computed with the ISORROPIA model (Nenes et al., 1999). Heterogeneous chemical processes on particles and fog droplets (nitrate production) and a simplified sulfur aqueous chemistry (sulfate production) have been implemented. Moreover, a preliminary chemical module describing the formation of secondary organic aerosols was introduced.

Meteorological data are provided by the National Center for Environmental Prediction (NCEP) analyses, refined by the 5th generation Pennsylvania State University model: MM5 (Dudhia, 1993), version 2.3.6. In order to have low computational cost, MM5 is used at the continental scale with a relatively low resolution (36 km) over a domain encompassing the CHIMERE

Table 1
Description of the simulations

Simulation name	Description
BC	Base simulation with all emissions
WP	Simulation without Paris basin emissions
WB	Simulation without Belgium emissions
WN	Simulation without The Netherlands emissions
WI	Simulation without Italy emissions
WF	Simulation without the whole France emissions

domain, with 25 vertical levels. At the local scale, a 5 km horizontal resolution is chosen.

In order to account for pollutants transported through the model domain boundaries, the continental runs are driven by GOCART model climatologies (Ginoux et al., 2001; Ginoux et al., 2004) for aerosol species, while the MOZART climatologies (Horowitz et al., 2003) are used for the gas-phase species. PM components at the boundaries include desert dust, organic and elemental carbon, and sulfates.

All simulations listed in Table 1 are run on the 10 February –31 March period. Results from 12 February are presented to leave a two days spin-up.

3. Emission inventory

The 2001 anthropogenic emission data from the EMEP database have been used for the continental runs (Vestreng et al., 2004). Annual emitted amounts of NO_x, CO, SO_x, NMVOC, NH₃, PPM₁₀ and PPM_{2.5} are available for 11 SNAP activity sectors. These data, initially provided by each country, are given on the EMEP grid (50 km resolution), following the methodology described in Vestreng (2003).

Calculation of model species emissions is made in several steps. First, the spatial emission distribution from the EMEP grid to the CHIMERE grid is performed using an intermediate fine grid at 1 km resolution. The knowledge of soil types on the fine grid allows for a better distribution of the emissions according to urban, rural, maritime and continental areas. This high-resolution land use inventory comes from the Global Land Cover Facility (GLCF) data set. Time profiles of NO_x, CO, SO_x and NMVOC are considered depending on SNAP activity sectors and are provided by the IER (University of Stuttgart). For NH₃, no time variability is considered. According to Aumont et al. (2003) HONO emission is set to 0.8% of NO_x

while NO₂ emission is set to 9.2% of NO_x emissions, the remaining NO_x emissions being NO. Afterwards, for each SNAP activity sector, the total NMVOC emission is split into emissions of 227 real individual NMVOC according to the AEAT speciation (AEAT, 2002). Finally, real species emissions are aggregated into model species emissions. For instance, the MELCHIOR chemical mechanism used in CHIMERE, accounts for 10 NMVOC. Mass-reactivity weighting of real emission data is done following the methodology of Middleton et al. (1990), so that the overall ozone production capability of the emission mixes is kept constant through the emission processing procedure.

For the local scale simulations over Ile-de-France area, the official emission inventory developed by the Paris air quality monitoring network AIRPARIF is used. This inventory is based on 2001 data, a detailed description is given in Hodzic et al. (2005).

4. Available observations

Two sites of the AIRPARIF air quality network have been equipped with monitoring instruments: a urban site near Paris, Gennevilliers (48°56'N, 2°18'E) and a rural site, Prunay (48°52'N, 1°40'E) located 50 km in the West side of Paris. Two kinds of PM₁₀ measurements are available during these episodes. A gravimetric method PARTISOL-Plus (daily data) and a routine method TEOM (hourly data). The PARTISOL-Plus has been assessed as an equivalent method compared to the EU reference method (EN 12341 standard). The TEOM method is a well-known method largely used in France; however, it is not considered as a standard method.

The PARTISOL filters were weighed using a micro-balance (Mettler Toledo MT5) with a sensitivity of ±1 µg. The used filters were stored in a room controlled in temperature (20±1°C) and relative humidity (50±3%) and equilibrated with these conditions for at least 24 h prior to weighing. The balance was first calibrated and zeroed and the electrostatic charges on the filters were eliminated using an ionization system (HAUG discharge system, multistat). Each filter was weighed three times and the mean of the three values was recorded with a standard deviation less than 4 µg. All filters were weighed again after 24 h to control possible bias. Two control filters were weighed during each weighing session and used to correct for weight changes in the sampled filters caused by variations in the balance room atmosphere. Sampling semi-volatile compounds in airborne particles is complicated by the fact that positive or negative artifacts (Solomon et al., 2003) may occur, due to volatilization during the sampling process or to adsorption of gaseous substances on deposited particles or on the filter material itself.

However, Chow et al. (1994) reported that losses of nitrate from the teflon filter are lower in winter (period of the study). Moreover, losses of semi-volatile compounds are minimized during the sampling process, by maintaining the sampler temperature near ambient conditions and conditioning the filters in a protective container during the transit to the laboratory at a temperature below 20 °C and storing the filters in a freezer after weighting.

A TEOM series 1400 was used in its standard configuration (Patasnick and Rupprecht, 1991). The TEOM filter was heated to 50 °C and correction factors were applied to the TEOM data ($b_0 = 3 \mu\text{gm}^{-3}$ and $b_1 = 1.03$). The same PM_{10} inlet-type used on the PARTISOL-Plus was used on the TEOM.

An other rural station, Fontainebleau (48°24'N, 2°42'E), is also used to evaluate PM_{10} (TEOM) and NO_2 model concentrations because measurements are not available at Prunay.

Sulfate, nitrate and ammonium daily measurements are available. Moreover, some size-segregated measurements have been carried out using a low-pressure LPI-30 Berner impactor (60 nm–16 μm) and Tedlar foils. Observations are presented for a small period in February 2003 in the form of raw data without inversion calculation of artifact corrections, e.g. the volatilization due to the low pressure.

5. Description of the pollution episodes

5.1. February 2003—episode EP1

Meteorological conditions are characterized by slight northeasterly winds over Paris due to a high-pressure zone in Scandinavia from the 13 to 18 March. The air mass is dry and cold in the North of France with highest temperatures close to 0 °C. Fig. 1 shows a back trajectory of an air parcel on Paris the 17 March. From the 19 to 20 March winds veer southeast, a low-pressure area appears on the Western coast of France. Thus, a cooler oceanic air mass comes in the northwest of France, increasing temperature and humidity. The 21 March in the morning, the situation is very stable with fogs in Normandy, high PM concentration levels are observed over the Paris area and in Belgium (confirmed by measurements and model results in Fig. 2). Winds turn southeast at the end of the episode. In this paper, the episode is called EP1, it is followed by nonpolluted conditions until 17 March.

5.2. March 2003—episodes EP2 and EP3

The second episode is similar to the previous one. From 13 to 20 March, an anticyclone over the Great Britain drives Northeasterly winds over the North of

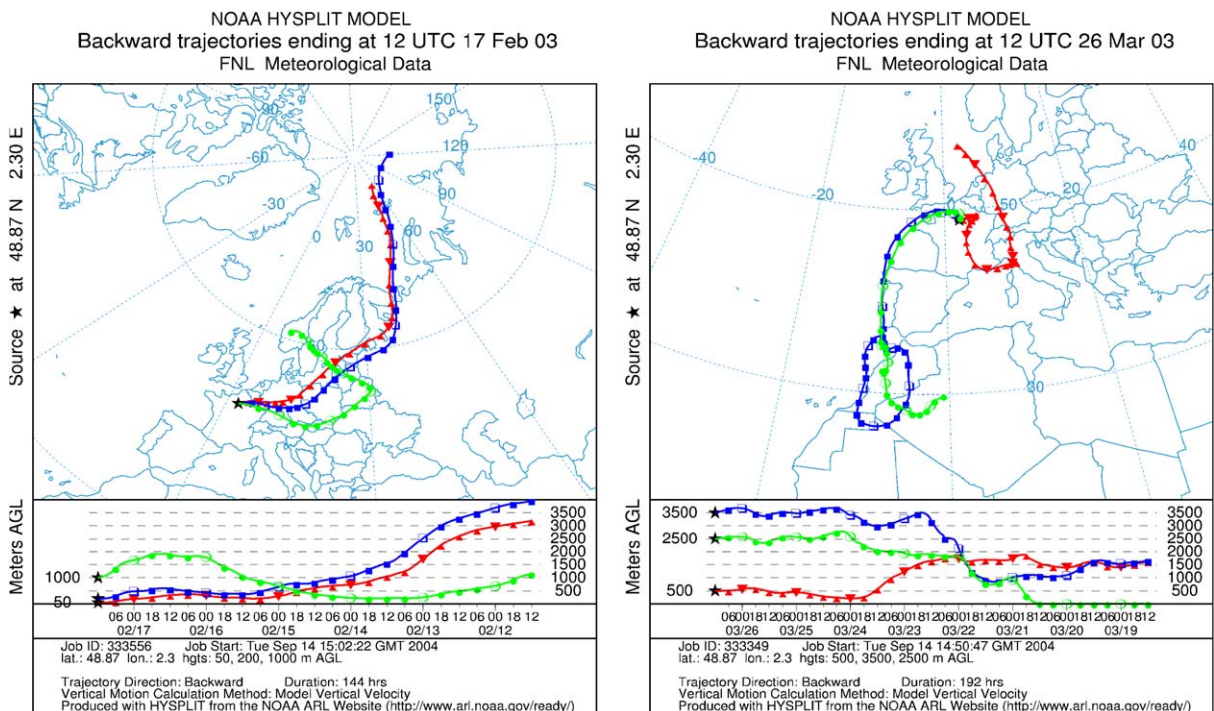


Fig. 1. Backward trajectory ending at 12:00 GMT over Paris on 17 February and 26 March, computed using NOAA HYSPLIT model and FNL meteorological data (courtesy of NOAA Air Resources Laboratory, <http://www.arl.noaa.gov>).

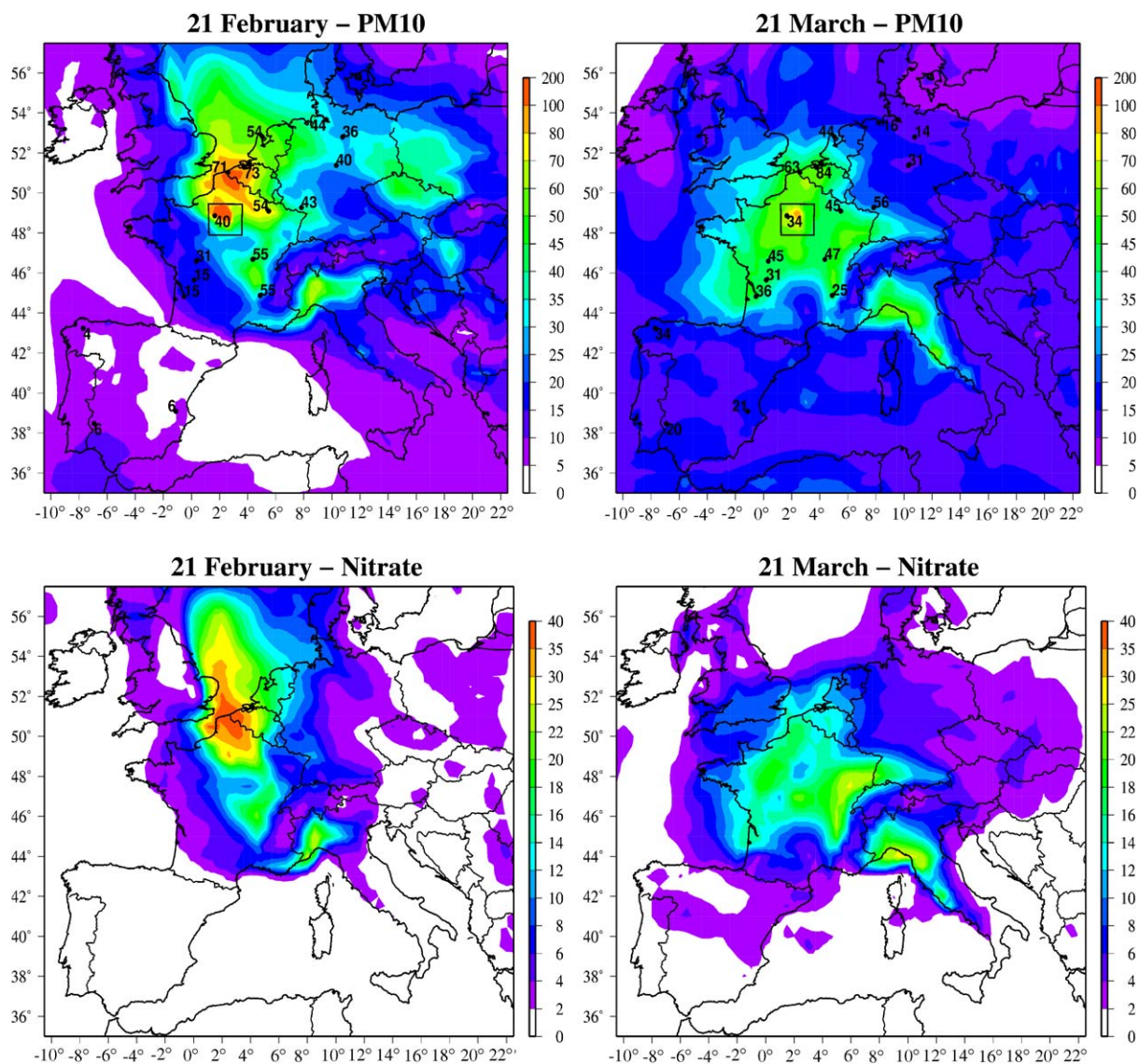


Fig. 2. Predicted PM₁₀ and nitrate daily mean concentrations at the continental scale (in $\mu\text{g m}^{-3}$) on 21 February and 21 March with PM₁₀ observed values (TEOM 50° C measurements in France). Values on the graphs (top panels) correspond to PM₁₀ observations (The TEOM instrument is used in France without corrections due to evaporation of the bulk phase).

France. Hazes and fogs are observed in Germany, Netherlands and Great Britain. In France, the atmosphere is dry at the beginning of the period and turns moist on the 18 March. On the 21 March, high humidity levels are observed on the Northwestern part of France up to the Paris region, winds are very weak, and high PM concentrations are observed. This episode is called EP2 in the following. Afterwards, Southerly winds generated by a low-pressure system on the Atlantic Ocean blow over the Western part of France.

A very stable situation occurs from 24 to 29 March (EP3) due to the high-pressure over Eastern Europe.

During this stagnant episode, on 26 March, an air mass comes from the Sahara towards the North of France at 2500 m in altitude (Fig. 1).

6. Simulation results against observations

6.1. Spatial representation of model results

In Fig. 2, daily mean PM₁₀ concentrations simulated over Europe on 21 February and 21 March are displayed together with some observations located at

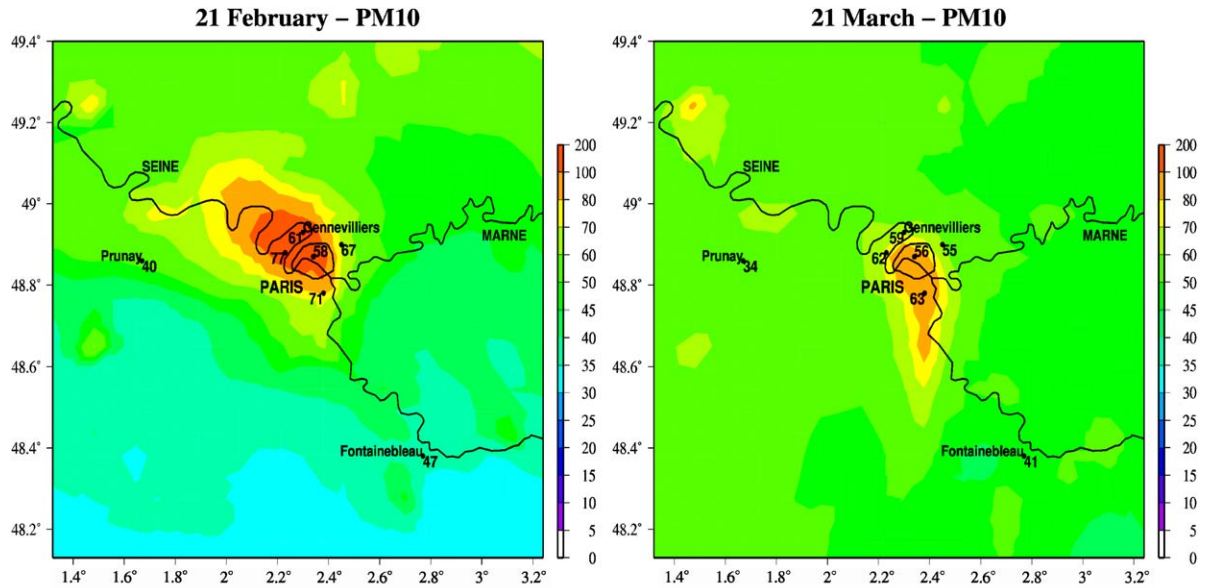


Fig. 3. Predicted PM₁₀ daily mean concentrations at the local scale (in $\mu\text{g m}^{-3}$) on 21 February and 21 March. Values on the graphs correspond to PM₁₀ observations (The TEOM instrument is used in France without corrections due to evaporation of the bulk phase).

Table 2

Error statistics based on hourly data for NO_x-NO, PM₁₀, and PM₁₀ without ammonium nitrate at Fontainebleau and Gennevilliers for the 12 February–31 March period

Simulation scale (resolution)	Pollutants	Fontainebleau					Gennevilliers				
		Obs. ^a	Mod. ^b	Corr. ^c	Nerr. ^d	Rms. ^e	Obs. ^a	Mod. ^b	Corr. ^c	Nerr. ^d	Rms. ^e
Local (~5 km) (AIRPARIF inventory)	PM ₁₀ -AN ^f	23.6	13.4	0.64	43.2	13.8	32.8	30.2	0.65	41.4	18.9
	PM ₁₀	23.6	23.0	0.63	39.4	10.8	32.8	40.8	0.67	56.1	23.6
	NO _x -NO ^g	18.4	12.2	0.61	41.0	11.6	57.6	56.4	0.75	29.2	19.7
Continental (~50 km) (EMEP inventory)	PM ₁₀ -AN ^f	23.6	19.5	0.65	32.6	11.5	32.8	35.1	0.64	48.3	18.7
	PM ₁₀	23.6	28.8	0.64	48.3	13.7	32.8	45.5	0.63	69.8	26.4
	NO _x -NO ^g	18.4	19.7	0.56	60.1	11.5	57.6	49.9	0.76	34.4	20.2

Statistics are reported for model results at the continental and local scales. Observed values for PM₁₀ and PM₁₀-AN are issued from the TEOM system.

^aObserved mean concentration ($\mu\text{g m}^{-3}$): TEOM data for PM₁₀.

^bMean predicted concentration ($\mu\text{g m}^{-3}$).

^cCorrelation.

^dNormalized error (%).

^eRoot mean square error ($\mu\text{g m}^{-3}$).

^fPM₁₀ (TEOM) without ammonium and nitrate.

^gNO_x-NO equivalent NO₂.

rural and near city sites. Measurements show background daily mean values exceeding $40 \mu\text{g m}^{-3}$ in a large part of Western Europe. The most striking feature in Fig. 2 is the apparent overestimation of the model in Prunay. In France, one has to keep in mind that PM₁₀ routine data are issued from TEOM 50 °C measurement system known to evaporate a large part of ammonium

nitrate. Indeed, according to the modeling results at the continental scale, these episodes seem correlated with high nitrate levels.

A zoom on Ile-de-France with the local scale version of CHIMERE is presented in Fig. 3, showing a PM pollution plume coming from Paris. These too-high predicted concentrations are mainly attributable to

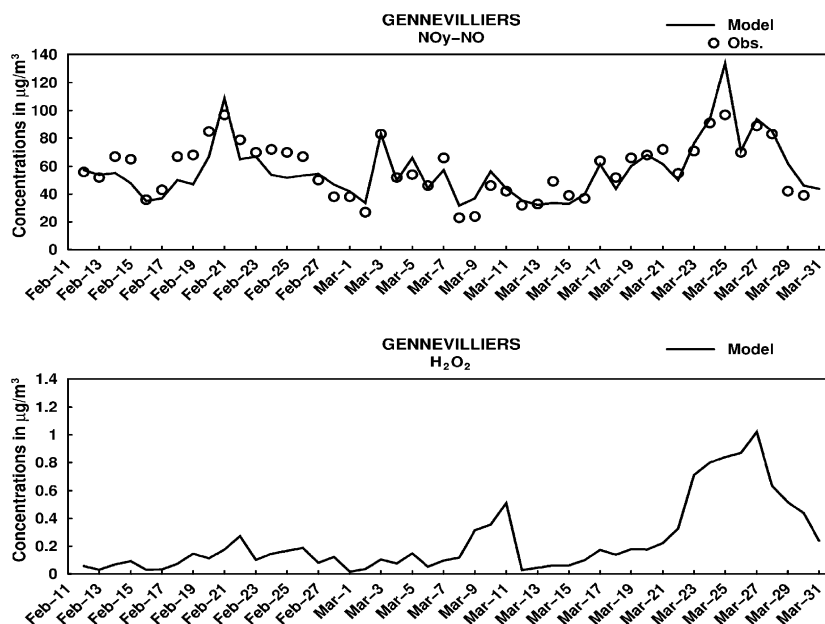


Fig. 4. Daily mean predicted concentrations for $\text{NO}_y\text{-NO}$ and H_2O_2 at Gennevilliers. Observations are reported for only $\text{NO}_y\text{-NO}$.

primary particles because the local inventory for PM is largely overestimated over the Paris city as demonstrated by Hodzic et al. (2005).

6.2. Transport and mixing processes

The pollutant $\text{NO}_y\text{-NO}$ is used to evaluate the transport and the mixing processes in the model. Actually, AIRPARIF measures $\text{NO}_y\text{-NO}$ concentrations as an equivalent observation for NO_2 . In Table 2, predicted $\text{NO}_y\text{-NO}$ concentrations using the local simulation against observed values indicate satisfactory error statistics for the whole period at Gennevilliers: a small absolute bias, a low normalized error with a correlation coefficient of 0.75. These good results are in agreement with the time series of NO_2 presented in Fig. 4. These results confirm that transport processes are well parameterized in the model for urban areas. At Fontainebleau, a significant negative bias is observed in Table 2. An overestimation of inversion layer heights and an underestimate of NO_x emissions for the local inventory in rural areas can explain this statement. In Table 2, the differences obtained on error statistics regarding the simulation scales show that the continental inventory is slightly overestimated in rural areas (Fontainebleau) with low scores for the continental model.

6.3. Particulate components

Due to the expected evaporation of ammonium nitrate, the PM_{10} measured with TEOM instrument is

expected to be comparable to the $\text{PM}_{10}\text{-AN}$ predicted concentrations (as $\text{PM}_{10}\text{-ammonium-nitrate}$) assuming that ammonium and nitrate are mainly under the ammonium nitrate form. With this assumption, error statistics are calculated, and the same scores as for $\text{NO}_y\text{-NO}$ are observed for $\text{PM}_{10}\text{-AN}$, they can be explained by following the same interpretation. The very large negative bias at Fontainebleau could also be due to missing biogenic-emitted species. When PM_{10} are directly compared to the TEOM values, the evaporation of ammonium nitrate is exhibited in Table 2 by a large positive bias. Regarding the influence of the resolution in Table 2, the continental model gives better results for $\text{PM}_{10}\text{-AN}$ at Fontainebleau (low-normalized error and bias) compared to the local simulation. The opposite is observed for the urban site Gennevilliers.

Time series at Prunay and Gennevilliers from 11 February to 31 March are presented in Fig. 5. The temporal evolution of ammonium and nitrate is quite fairly reproduced at Gennevilliers and Prunay. However, observed concentrations are globally underestimated by the model. During the episodes, the mass ratio nitrate/ammonium ≈ 3 (close to the theoretical ratio of the molar masses: 3.4) and the weak values of sulfate concentrations confirm the presence of ammonium nitrate in particles. For sulfate, observations are not very well predicted. Indeed, the aqueous chemistry depends on pH (estimated by the model), on the liquid water content (a parameter difficult to compute in meteorological models) and H_2O_2 concentrations. The H_2O_2 concentration levels

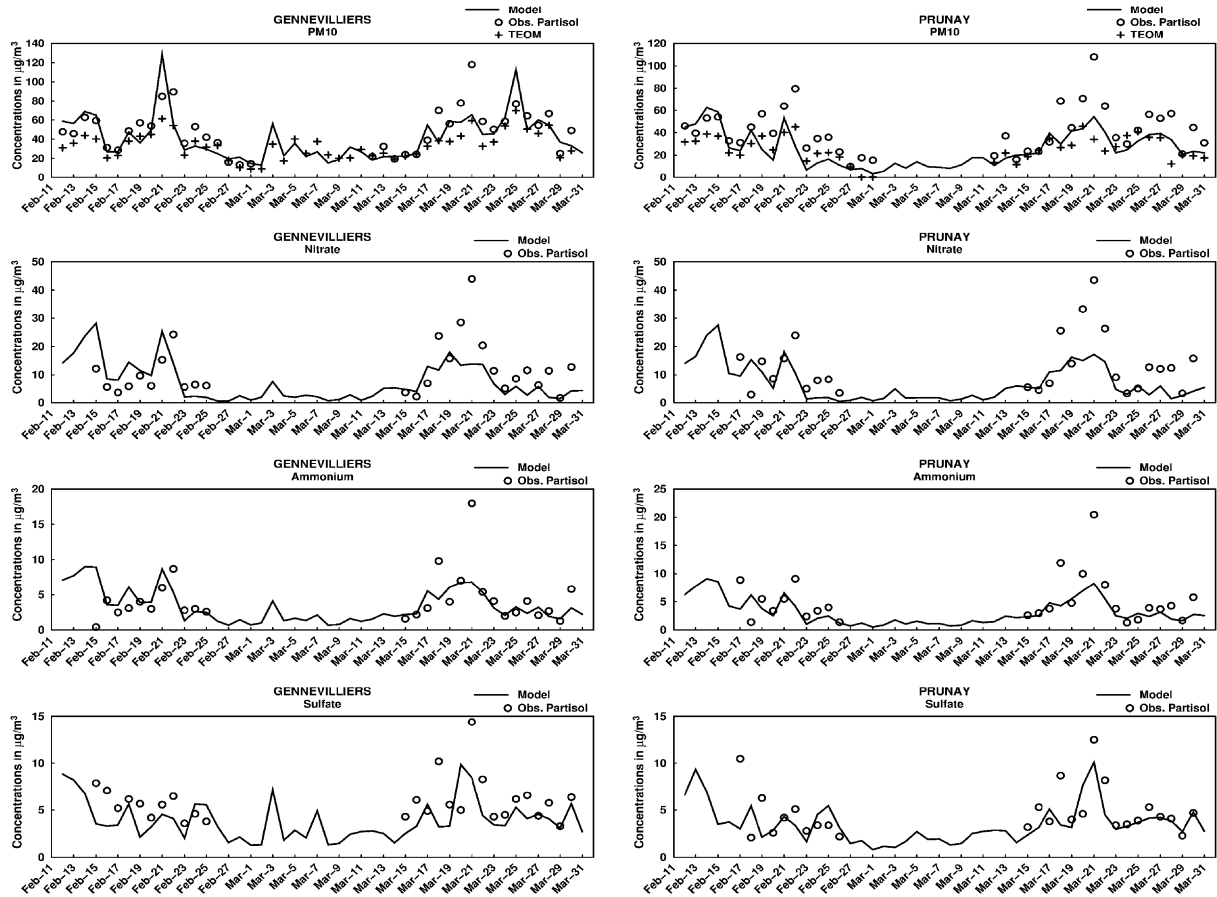


Fig. 5. Daily mean predicted concentrations versus observations for PM₁₀, Nitrate and ammonium at Prunay and Gennevilliers.

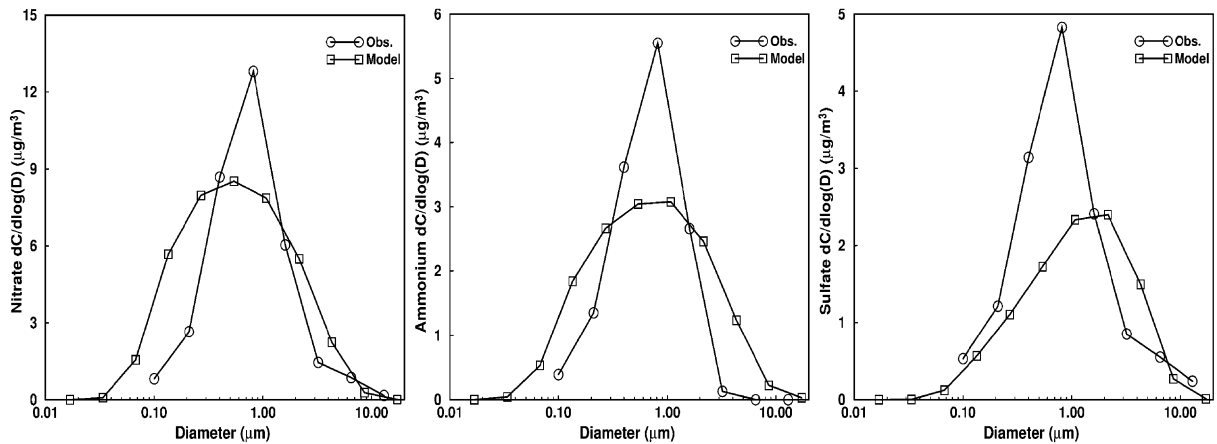


Fig. 6. Mean spectral distribution of ammonium, nitrate and sulfate from 19 February 16h GMT to 21 February 10h GMT at Gennevilliers (as aerodynamic diameter assuming a particle density of 1.5 g cm^{-3} in the model).

showed in Fig. 4 are of the same order of magnitude as the ones reported by Sakugawa et al. (1990) for urban areas in winter.

In Fig. 5, a good temporal correlation is observed for PM₁₀ at Gennevilliers, particularly with PARTISOL data. Simulation results show a peak on 21 February,

due to the overestimate of concentrations coming from the Paris city as described in Section 6.1. The underestimate of predicted PM₁₀ the 18 and 21 March is correlated with a large underestimate of nitrate and ammonium, primary particle concentrations could also be underestimated. The global underestimation of PM concentrations is due to a lack of ammonium nitrate production or advection at the continental scale. Compared to other PM pollution events, EP3 measure-

ments display weak nitrate and ammonium concentrations particularly at Gennevilliers.

6.4. Size distribution

Evaluating an aerosol model requires information on the size distributions of the main components. The mean diameter for sulfate, nitrate and ammonium distribution for a 3-day period in February 2003 is in the range

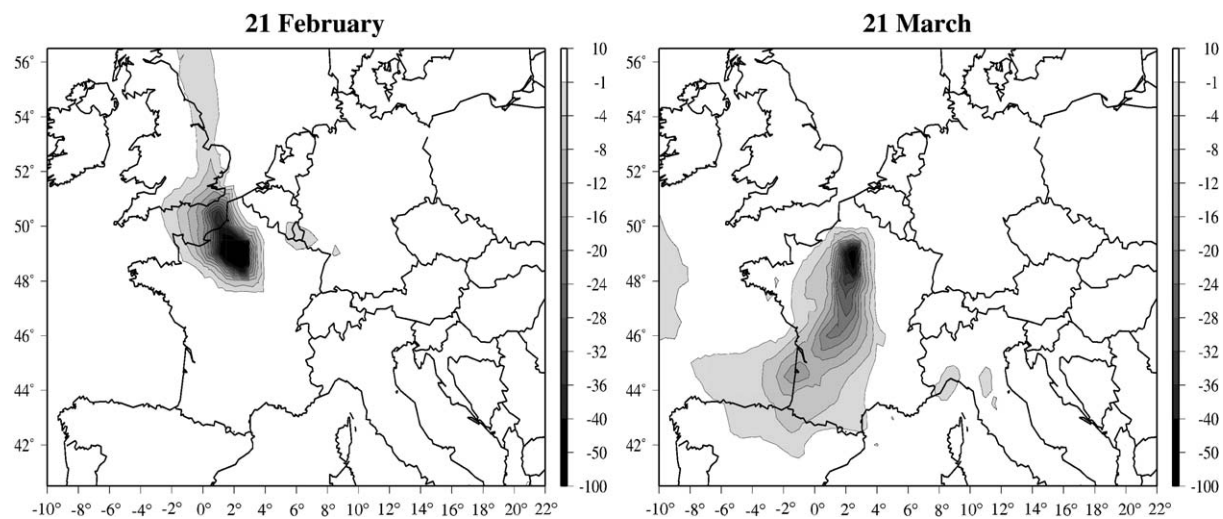


Fig. 7. PM₁₀ model concentration decreases without the Paris Basin anthropogenic emissions ($\mu\text{g m}^{-3}$) on 21 February (left panel) and 21 March (right panel).

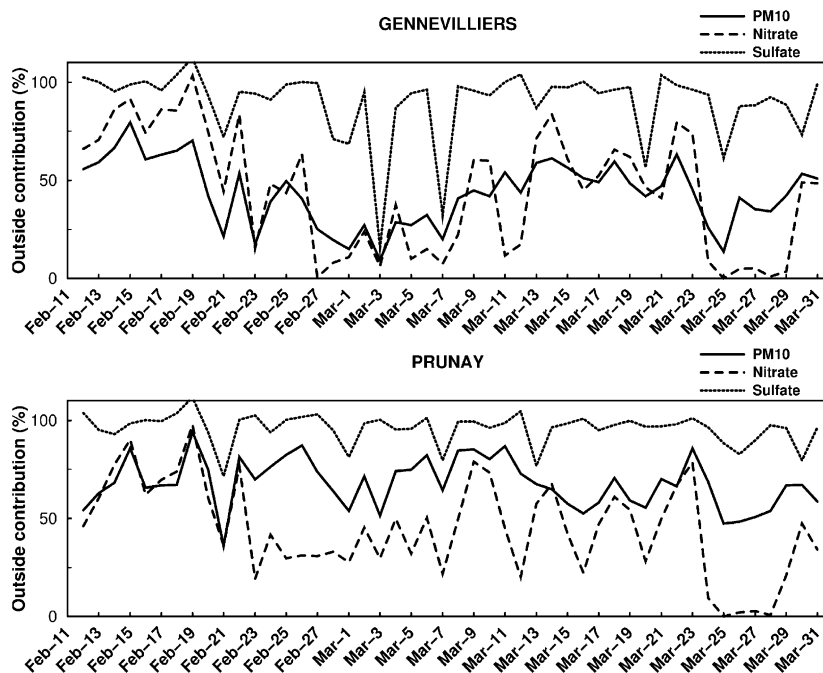


Fig. 8. Outside contribution (in %) of PM₁₀ concentrations on the Paris Basin domain.

0.7–0.9 μm (Fig. 6), all these species absorb onto fine particles. Model results are in good agreement with observations but model spectral distributions are wider than the observed ones. The numerical diffusion generally due to the sectional approach could explain such a behavior (Zhang et al., 1999).

Modeling results confirm that differences between TEOM and PARTISOL measurements during these events are largely explained by ammonium nitrate volatilization induced by the TEOM measurement procedure. Such model studies give information on the spatialization of PM pollution events and the chemical characteristic of particles. As an example, a simulated map of ammonium nitrate concentrations is useful to identify the regions concerned by the differences expected by the two PM measurement methods. In the present study, model results show that most of the episodes over Ile-de-France also affect a large part of Western Europe. The question of

the origin of such wintertime episodes is treated in the next section.

7. Analyses on emissions

7.1. Methodology

In this section, sensitivity analyses are carried out on anthropogenic emissions. The principle is the following: emissions of a specific area A are completely removed and the resulting influence on PM concentrations elsewhere is observed. The idea is to compare a base case scenario with all emissions (BC) to a particular test case (WA) without emissions in area A (a country or a subdomain). Modeling results have to be carefully interpreted; the difference Δ of the concentrations between two simulations (WA–BC) gives information about the impact of area A on concentrations at point P, but not the real

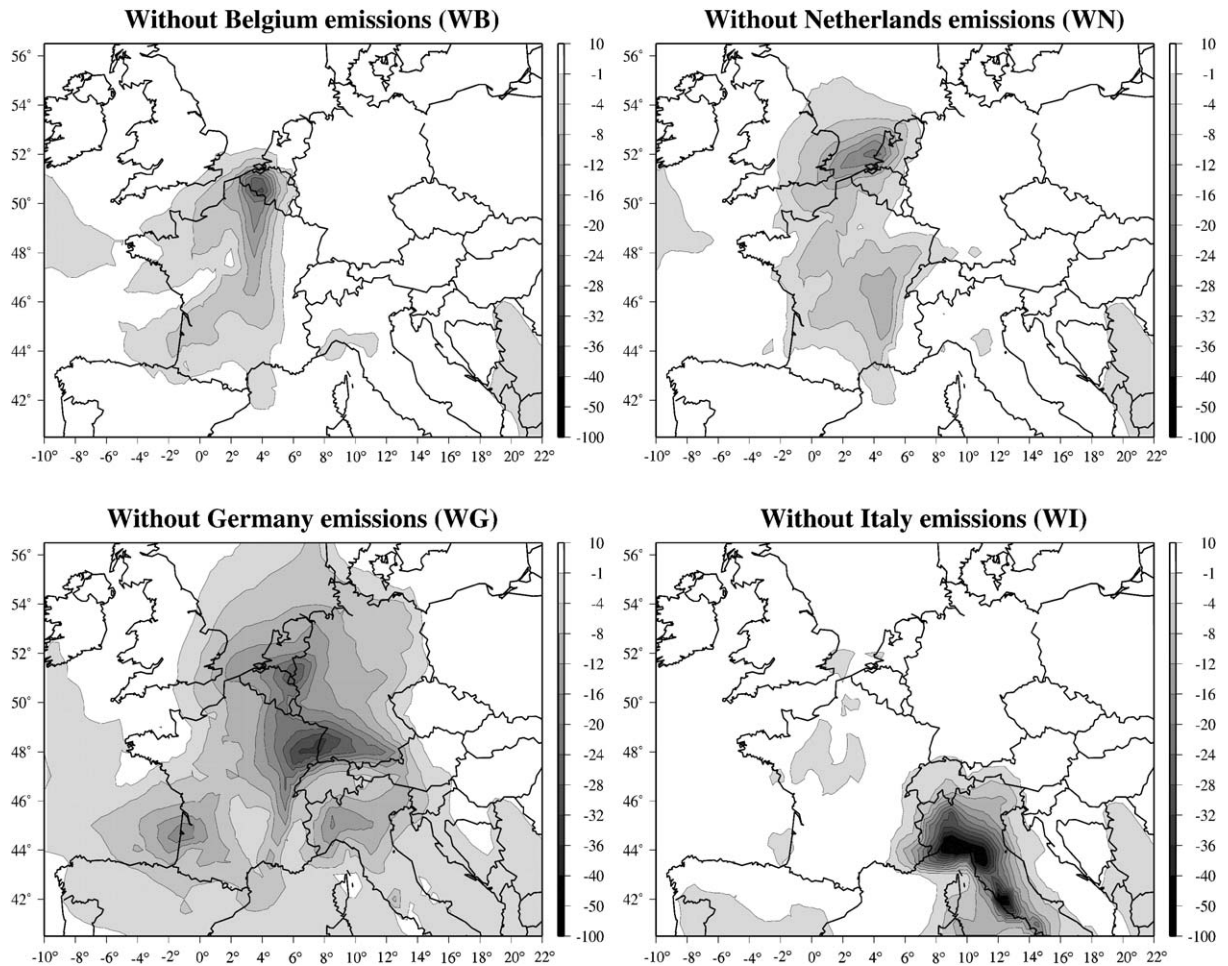


Fig. 9. Spatial representation of PM₁₀ daily mean concentration differences ($\mu\text{g m}^{-3}$) between simulations without country emissions (WB, WN, WG, WI) and the base case (BC) on 21 March.

quantity directly coming from A. For instance, local nitric acid produced at the point P can be neutralized by ammonia emitted in zone A and transported at point P. Therefore, the resulting ammonium nitrate in particles can have two distinct origins.

This way of performing such analyses must be improved by marking all component emissions of each source, but this methodology implies non-realistic computation times. In the next subsections, influences of the Paris Basin, Germany, Netherlands, Belgium and France are discussed.

7.2. Evaluation of the PM continental transport over the Paris Basin

A first step consists in evaluating the impact of PM continental transport over the Paris Basin during the pollution events described previously. Anthropogenic PM and gas emission sources are removed in the Paris Basin. Therefore, the predicted concentrations within the domain are representative of concentrations coming from outside. Of course, this approach also allows for the quantifica-

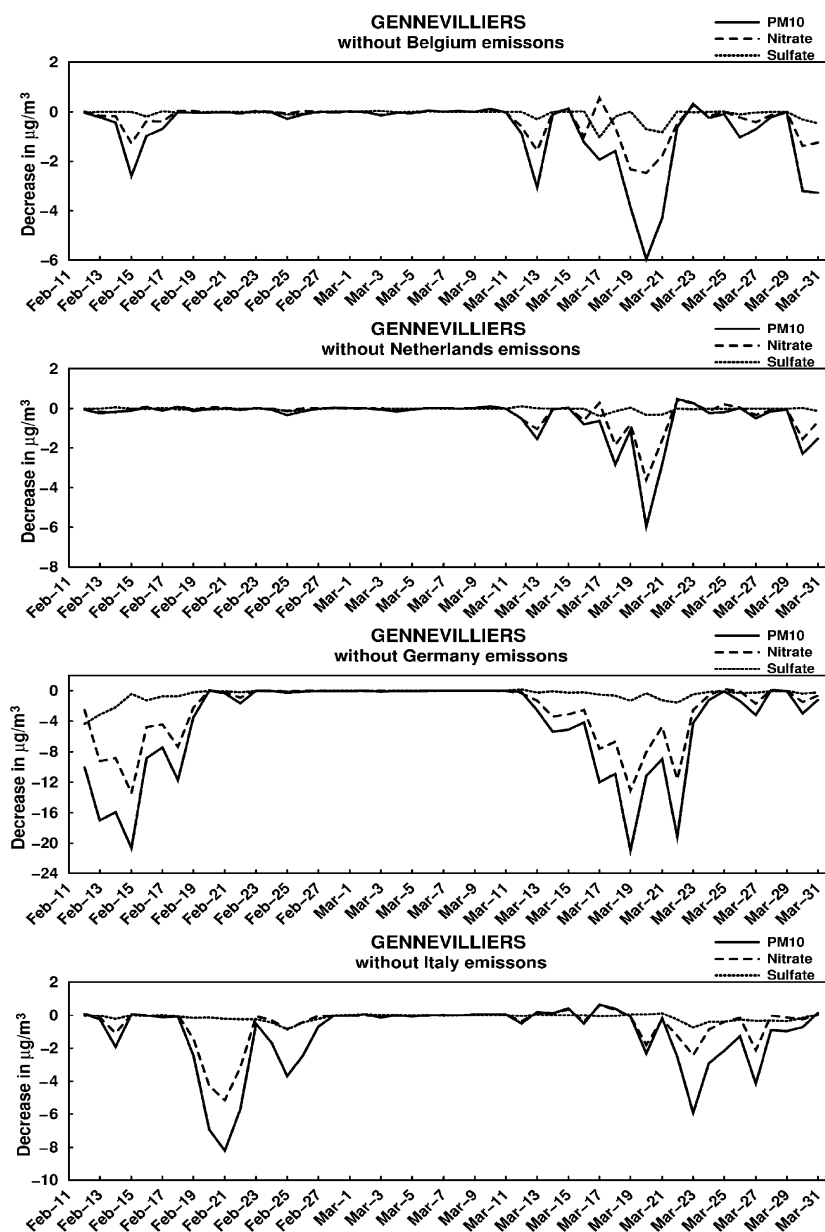


Fig. 10. Temporal variation of the differences Δ ($\mu\text{g m}^{-3}$) between WB, WN, WG, WI simulations and the BC.

tion of the impact of Ile-de-France emissions on the rest of France.

With the notations defined in Table 1 for the simulation WP and BC, Fig. 7 displays the spatial patterns of the differences Δ as previously defined by

$$\begin{aligned} & (\text{PM}_{10}\text{concentrations from WP simulation}) \\ & - (\text{PM}_{10}\text{concentrations from BC simulation}). \end{aligned}$$

During EP1 the 21 February, Paris emissions seem to have an impact on the PM concentrations in the southeast of The United Kingdom (up to $10\mu\text{g m}^{-3}$). That corresponds to a traditional situation following a PM accumulation over the North of France during stable pollution episodes. A southeast flux in front of a low-pressure system over the Atlantic Ocean drives pollutant towards United Kingdom. On 21 March, it is noteworthy that Paris emissions have a strong impact on PM_{10} concentrations in the southwest of France ($10\text{--}12\mu\text{g m}^{-3}$), hundreds of kilometers further, essentially due to ammonium nitrate formation.

To analyze the Paris Basin concentrations, the outside Paris Basin contribution is expressed by $100 \times C_{\text{WP}}/C_{\text{BC}}$ (in %) with C_{WP} and C_{BC} , respectively, the concentrations for the WP and BC simulations.

This ratio can theoretically exceed 100% because of nonlinearities in the model. The temporal variability of the ratio for sulfate, nitrate and PM_{10} is presented in Fig. 8. Sulfate observed at Gennevilliers and Prunay generally comes from outside the Ile-de-France domain, but concentrations remain low (usually less than $5\mu\text{g m}^{-3}$). Nitrate and ammonium come from outside during the first two episodes with an average contribution often exceeding 50%. For PM_{10} , the outside

contribution largely exceeds most of the time 50% at Prunay and sometimes 80%. The contribution is less important in Gennevilliers (urban site) due to important local PPM emissions and is usually in the range (20–50%) with the highest values during pollution events.

For the last episode, EP3, PM_{10} concentrations over the Paris Basin are locally produced (ammonium nitrate) or emitted (PPM). The outside contribution of PM_{10} is close to 30%.

The relative contribution of local and continental sources to the pollution episodes have been quantified. The origin of such PM events is investigated hereafter.

7.3. Possible origin of wintertime PM pollution episodes over Paris in February and March 2003

7.3.1. European origin?

As previously done, the influence of neighboring countries over the Paris Basin concentrations is assessed. Influences of Belgium, Netherlands, Germany and Italy are studied. Because of their location, these countries are likely to have an influence over the PM concentrations on the North part of France during such episodes. Thus, emissions of these countries are removed by turns (Table 1). Only results for 21 March are presented, this episode covering a very large part of Western Europe. The PM_{10} concentration difference Δ for the case “without Italy emissions” is defined by

$$\begin{aligned} & (\text{PM}_{10}\text{concentrations from WI simulation}) \\ & - (\text{PM}_{10}\text{concentrations from BC simulation}) \end{aligned}$$

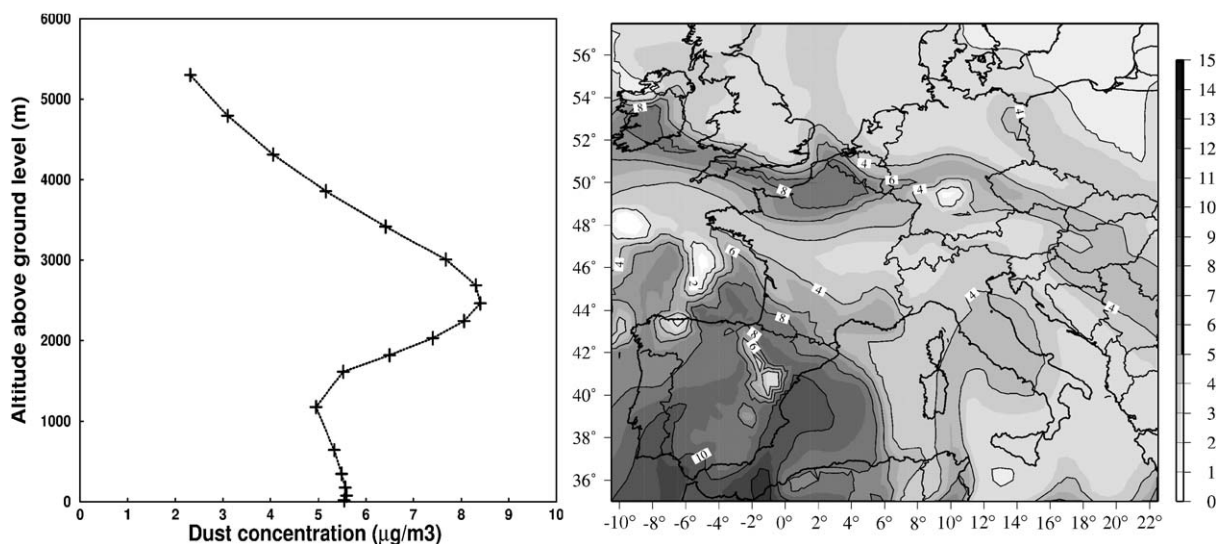


Fig. 11. Left panel: simulated dust profile the 26 March 2003 12:00 GMT by CHIMERE, right panel: simulated dust concentrations ($\mu\text{g m}^{-3}$) around 2500m in altitude on 26 March at 12:00 GMT with a 18-level model version.

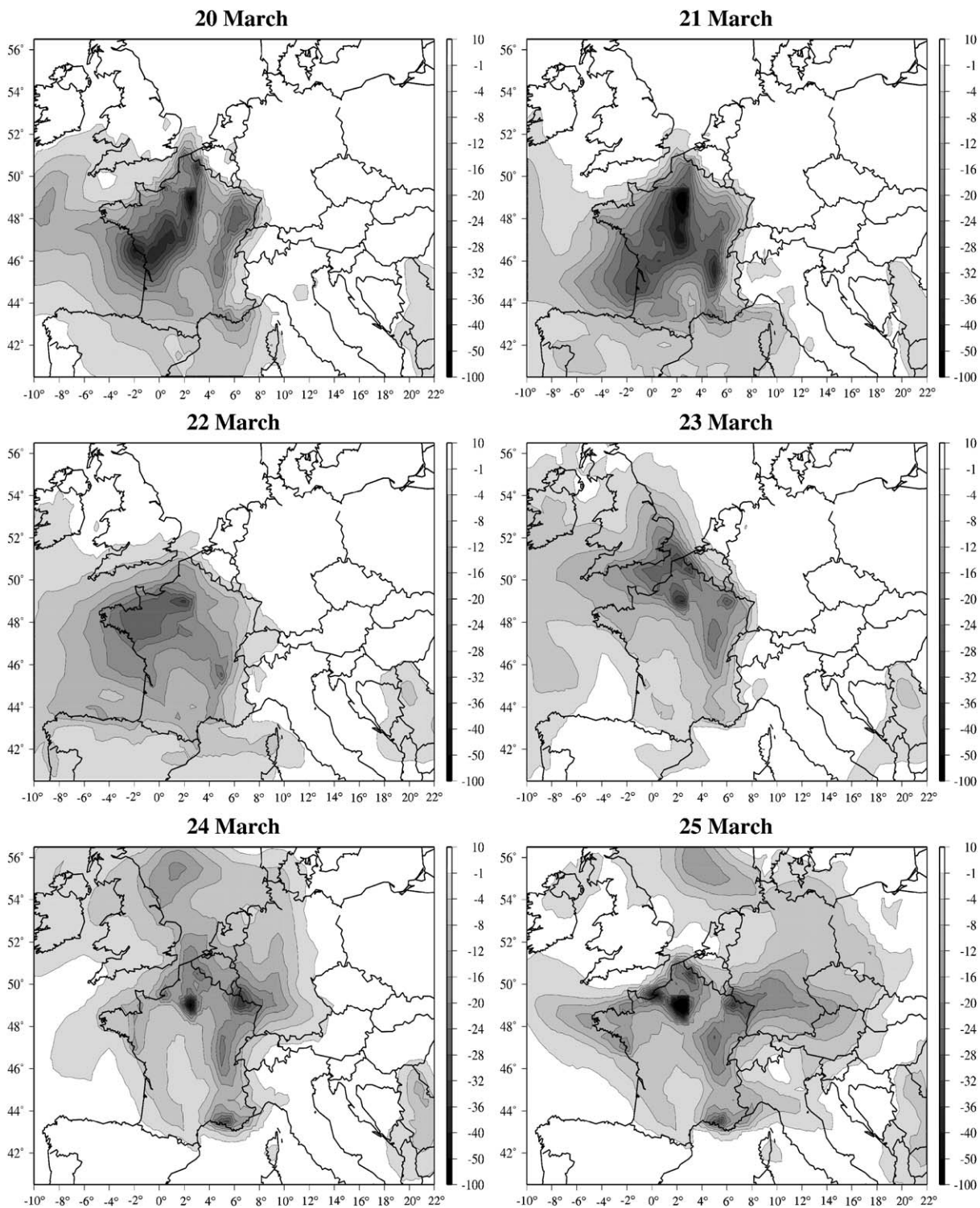


Fig. 12. PM₁₀ daily mean concentration differences between simulations without French emissions and the BC from 20 to 25 March.

and so on, for the other cases presented in Table 1. In Fig. 9, results are presented for each country. The influence of Belgium emissions spreads out from the North up to the southwest of France. A decrease of $10\text{--}15\ \mu\text{g m}^{-3}$ in PM concentrations is observed close to Belgium and about $5\ \mu\text{g m}^{-3}$ up to the southwest of France. For the Dutch contribution, it is quite different: the influence seems most important in the South part of France near Lyon. Ammonia from The Netherlands is transported in these regions and can react with nitric acid locally produced, to form ammonium nitrate. Germany seems to have the most significant impact over the northeast and southwest of France, while Italy emissions have solely an influence in the very south-eastern part of France.

In Fig. 10, the temporal variation of Δ for each country at Gennevilliers is presented. For EP1, only Germany contributes significantly to PM_{10} concentrations near Paris (up to $20\ \mu\text{g m}^{-3}$) until the 20 February. Belgium and The Netherlands have a weak influence ($<2\ \mu\text{g m}^{-3}$). The influence of Italy is important on 21 February (up to $10\ \mu\text{g m}^{-3}$). For EP2, Germany, Netherlands and Belgium impact significantly (between 6 and $20\ \mu\text{g m}^{-3}$), and as for EP1, Italy brings a contribution the days after. Generally, Italy has a specific effect compared to other countries. Its geographic location involves a time-shifted effect when the northeast flux turns southeast over Paris. As discussed in the previous section, Fig. 10 confirms the local origin of the EP3 event, with only few $\mu\text{g m}^{-3}$ of PM concentrations due to surrounding countries on 24–29 March.

7.3.2. Extra European origin?

On 24–29 March, Southerly winds blow over the Atlantic Ocean with an air mass directly coming from Sahara. Hodzic et al. (2004) already observed with Lidar measurements near Paris a thin PM layer at 2500 m above the ground level suspected to be desert dusts. In Fig. 11, the simulated dust concentrations ($\mu\text{g m}^{-3}$) at 2500 m in altitude on 26 March at 12:00 GMT over the domain is presented. A dust layer is observed from Ireland to the North of France. This particular episode has been simulated with a 18-levels model version. The ability of the model to simulate the correct altitude of this dust layer (Fig. 11) can be noticed. As described in Rodriguez et al. (2001), wintertime dust outbreaks in the South of Europe (Spain and Portugal) are classically due to the cyclonic activity over the Atlantic as shown with EP3. Unfortunately, no specific measurements highlighting the desert dust contribution were available. According to model results at the ground level, desert dusts should contribute to a minor extent to the PM load (about $5\ \mu\text{g m}^{-3}$). However, the dust concentrations are certainly underestimated. Actually, as GOCART runs for year 2003 were not available at the time of the present study, and as hourly or even daily boundary

conditions were quite uneasy to process, the average of monthly mean values taken from runs over years 2000 and 2001 was used. Since dust events are very sporadic during the year, boundary conditions for dusts are tuned (reduced by a factor of 3) to be representative of the dust background level (Vautard et al., 2005). In doing so, dust outbreaks in Europe are expected to be underestimated, then it is difficult to conclude on the influence of this event on the EP3 episode.

7.3.3. Influence of France

A simulation without French emissions was run to assess their influence during episodes. Modeling results in Fig. 12 display the spatial pattern of the results from 20 to 25 March. At the height of the episode, on 20–22 March, French emissions have only an influence on Spain (up to $10\ \mu\text{g m}^{-3}$ on the North of Spain), the main plume extending over the Atlantic Ocean. When the Northeasterly flux veers southeast at the end of the event, as it was the case for Italy, the plume extends northwest up to Ireland through Great Britain during on 23 March. Afterwards, the plume structure disappears. Nevertheless, the influence of France emissions remain significant up to Eastern Europe, close to $10\text{--}15\ \mu\text{g m}^{-3}$ in Germany, Netherlands and Belgium.

8. Conclusions

The CHIMERE model has been used over Europe with a zoom on the Paris Basin. Wintertime PM pollution episodes during February and March 2003 were studied. Firstly, a model evaluation was carried out to assess model performances. TEOM and PARTISOL measurements display large differences due to ammonium nitrate evaporation in the TEOM system processes. Although model results are quite good for PARTISOL PM_{10} , ammonium and nitrates concentrations, model deficiencies are observed for sulfate. Indeed, sulfate in winter is produced in clouds, involving modeling parameters, which are sometimes difficult to obtain from meteorological outputs. Error statistics show large differences between the continental and local simulations due to the resolution and the two different inventories used.

Most of these episodes seem to have a continental origin, and the selected approach attempts to estimate the advected part from outside Paris Basin to the total PM concentrations. On 21 February and 21 March episodes, the outside contribution reaches 50%, while during nonepisode situations the contribution drops down to 20%. When the episode reaches maximum concentrations, the “PM outside contribution” is mainly composed of ammonium nitrate. During 24–29 March, although a dust layer was observed and simulated by the model at 2500 m above ground level, the modeling study

confirms the local character of the pollution episode, essentially due to primary particle material emitted in the Paris area.

In the last section, the origin of the outside Paris contribution is investigated. A very preliminary sensitivity study is performed, by removing the emissions of the neighboring countries supposed to influence PM concentrations over Paris area. Germany, The Netherlands and Belgium seem to have a strong impact during EP1 and EP2. To a minor extent, Italy has an influence at the end of the episodes when the northeast flux veers southeast.

Removing all French anthropogenic emissions allows to assess the influence of French emissions on PM concentrations observed in the rest of Europe. During the studied episodes, France has only an influence on Spain. But at the end of the episodes, when the northeast flux veers southeast and west, France has successively a significant influence on PM concentrations in Great Britain, Belgium, Netherlands, Germany and up to Eastern Europe to a lesser extent.

Acknowledgements

This work has been financially supported by the French Environment Ministry (MEDD—Ministère de l'Écologie et du Développement Durable). The authors thank the Max-Planck Institute (Hamburg, Germany), M. Schultz, C. Granier, G. Brasseur and D. Niehl for graciously providing us with MOZART data. We also thank Paul Ginoux and Mian Chin (NASA, USA) for their contribution in the GOCART model simulations. We greatly thank the RIVM (Netherlands), U. Dauert (UBA, Germany), F. Fierens (IRCELINE, Belgium) and A. González (Ministerio de Medio Ambiente, Spain) for leaving us to have access to the air quality PM₁₀ data. The authors thank C. Honoré and R. Aujay (INERIS, France) for their scientific support. We also acknowledge R. Vautard (IPSL/CNRS, France) for providing us meteorological fields.

References

- Ackermann, I.J., Hass, H., Memmesheimer, M., Ebel, A., Binkowski, F.S., Shankar, U., 1998. Modal aerosol dynamics model for Europe: development and first applications. *Atmospheric Environment* 32, 2981–2999.
- AEAT/ENV/R/0545 Report, 2002. Speciation of UK emissions of NMVOC, Passant, N.R. February.
- Allen, G., Sioutas, C., Koutrakis, P., Reiss, R., Lurmann, F.W., Roberts, P.T., 1997. Evaluation of the TEOM method for measurement of ambient particulate mass in urban areas. *Journal of Air and Waste Management Association* 47, 682–689.
- Aumont, B., Chervier, F., Laval, S., 2003. Contribution of HONO sources to the NO_x/HO_x/O₃ chemistry in the polluted boundary layer. *Atmospheric Environment* 37, 487–498.
- Bessagnet, B., Rosset, R., 2001. Fractal modelling of carbonaceous aerosols—application to car exhaust plumes. *Atmospheric Environment* 35, 4751–4762.
- Bessagnet, B., Hodzic, A., Vautard, R., Beekmann, M., Cheinet, S., Honoré, C., Liousse, C., Rouil, L., 2004. Aerosol modeling with CHIMERE—preliminary evaluation at the continental scale. *Atmospheric Environment* 38, 2803–2817.
- Chow, J.C., Fujita, E.M., Watson, J.G., Lu, Z., Lawson, D.R., Ashbaugh, L.L., 1994. Evaluation of filter-based aerosol measurements during the 1987 Southern California air quality study. *Environmental Monitor and Assessment* 30, 49–80.
- Dudhia, J., 1993. A nonhydrostatic version of the Penn State/NCAR mesoscale model: validation tests and simulation of an Atlantic cyclone and clod front. *Monitoring Weather Review* 121, 1493–1513.
- EPA, 2004. Air Quality Criteria for PM. www.epa.gov.
- Gelbard, F., Seinfeld, J.H., 1980. Simulation of multicomponent aerosol dynamics. *Journal of colloid and Interface Science* 78, 485–501.
- Ginoux, P., Chin, M., Tegen, I., Prospero, J.M., Holben, B., Dubovik, O., Lin, S.-J., 2001. Sources and distributions of dust aerosols simulated with the GOCART model. *Journal of Geophysical Research* 106, 20255–20273.
- Ginoux, P., Prospero, J.M., Torres, O., Chin, M., 2004. Long term simulation of dust distribution with the GOCART model: correlation with the North Atlantic Oscillation. *Environmental Modeling and Software* 19, 113–128.
- Hodzic, A., Chepfer, H., Vautard, R., Chazette, P., Beekmann, M., Bessagnet, B., Chatenet, B., Cuesta, J., Drobinski, P., Goloub, P., Haeffelin, M., Morille, Y., 2004. Comparison of aerosol chemistry transport model simulations with lidar and Sun photometer observations at a site near Paris. *Journal of Geophysical Research* 109, D23201.
- Hodzic, A., Vautard, R., Bessagnet, B., Lattuati, M., Moreto, F., 2005. Long term urban aerosol simulation versus routine particulate matter observations. *Atmospheric Environment* (Accepted in).
- Horowitz, L.W., Walters, S., Mauzeralles, D.Z., Emmonds, L.K., Rasch, P.J., Granier, C., Tie, X., Lamarque, J.F., Schultz, M.G., Brasseur, J.P., 2003. A global simulation of tropospheric ozone and related tracers: description and evaluation of MOZART, version 2. *Journal of Geophysical Research* 108 (D24), 4784.
- Jacobson, M.J., 1997. Development and application of a new air pollution modelling system—Part III. Aerosol phase simulations. *Atmospheric Environment* 31, 587–608.
- Katsouyanni, I., Touloumi, G., Spix, C., Schwartz, J., Balducci, F., Medina, S., et al., 1997. Short term effects of ambient sulphur dioxide and particulate matter on mortality in 12 European cities: results from time-series data from the APHEA project. *BMJ* 314, 1658–1663.
- Meng, Z., Dabdub, D., Seinfeld, J.H., 1998. Size-resolved and chemically resolved model of atmospheric aerosol dynamics. *Journal of Geophysical Research* 103, 3419–3435.
- Middleton, P., Stockwell, W.R., Carter, W.P., 1990. Aggregation and analysis of volatile organic compound emissions for regional modelling. *Atmospheric Environment* 24, 1107–1133.

- Nenes, A., Pilinis, C., Pandis, S.N., 1999. Continued development and testing of a new thermodynamic aerosol module for urban and regional air quality models. *Atmospheric Environment* 33, 1553–1560.
- Pai, P., Vijayaraghavan, K., Seigneur, C., 2000. Particulate matter modeling in the Los Angeles basin using SAQM-AERO. *Journal of Air and Waste Management Association* 50, 32–42.
- Patasnick, H., Rupprecht, E.G., 1991. Continuous PM-10 measurement using the tapered element oscillating microbalance. *Journal of the Air and Waste Management Association* 41, 1079–1083.
- Pope, C.A., Burnett, R.T., Thun, M.J., Calle, E.E., Krewski, D., Ito, K., Thurston, G.D., 2002. Lung cancer, cardiovascular mortality, and long-term exposure to fine particulate air pollution. *JAMA* 287, 1132–1141.
- Rodriguez, S., Querol, X., Alastuey, A., Kallos, G., Kakaliagou, O., 2001. Saharan dust contribution to PM₁₀ and TSP levels in Southern and Eastern Spain. *Atmospheric Environment* 35, 2433–2447.
- Sakugawa, H., Kaplan, I.R., Tsai, W., Cohen, Y., 1990. Atmospheric hydrogen peroxide. *Environmental Science and Technology* 24, 1452–1461.
- Seigneur, C., 2001. Current status of air quality models for particulate matter. *Journal of Air and Waste Management Association* 51, 1508–1521.
- Schmidt, H., Derognat, C., Vautard, R., Beekmann, M., 2001. A comparison of simulated and observed ozone mixing ratios for the summer of 1998 in Western Europe. *Atmospheric Environment* 35, 6277–6297.
- Solomon, P., Baumann, K., Edgerton, E., Tanner, R., Eatough, D., Modey, W., Maring, H., Savoie, D., Natarajan, S., Meyer, M.B., Norris, G., 2003. Comparison of integrated samplers for mass and composition during the 1999 Atlanta Supersites project. *Journal of Geophysical Research* 108 (D7), 8423.
- Vautard, R., Martin, D., Beekmann, M., Drobinski, P., Friedrich, R., Jaubertie, A., Kley, D., Lattuati, M., Moral, P., Neining, B., Theloke, J., 2003. Paris emission inventory diagnostics from ESQUIF airborne measurements and a chemistry transport model. *Journal of Geophysical Research* 108 (D17).
- Vautard, R., Bessagnet, B., Chin, M., Menut, L., 2005. On the contribution of natural Aeolian sources to particulate matter concentrations in Europe: testing hypotheses with a modelling approach. *Atmospheric Environment* 39, 3291–3303.
- Vestreng, V., 2003. EMEP/MSW Technical Report. Review and Revision. Emission data reported to CLRTAP. MSW Status Report 2003. EMEP/MSW Note 1/2003. ISSN 0804-2446.
- Vestreng, V., et al., 2004. Inventory Review 2004, Emission Data reported to CLRTAP and under the NEC Directive, EMEP/EEA Joint Review Report, EMEP/MSW Note 1/2004. ISSN 0804-2446.
- Warren, D.R., 1986. Nucleation and growth of aerosols. Thesis of the California Institute of Technology, Pasadena.
- WHO report, 2003. Health aspects of air pollution with particulate matter, ozone and nitrogen dioxide. Report on a WHO Working Group Bonn, EUR/03/5042688, Germany 13–15 January 2003.
- Zhang, Y., Seigneur, C., Seinfeld, J.H., Jacobson, M.Z., Binkowski, F., 1999. Simulation of aerosol dynamics: a comparative review of algorithms used in air quality model. *Aerosol Sciences Technology* 31, 487–514.